BROOKHAVEN
NATIONAL LABORATORY

Interstrand Resistance in Cored Rutherford-Type Superconducting Cables

Rainer Soika and Arup K. Ghosh

August 2004

Superconducting Magnet Division

Brookhaven National Laboratory
P.O. Box 5000
Upton, NY 11973-5000
www.bnl.gov

Managed by
Brookhaven Science Associates, LLC
for the United States Department of Energy under
Contract No. DE-AC02-98CH10886

DISCLAIMER

This report was prepared as an account of work sponsored by an agency of the United States Government. Neither the United States Government nor any agency thereof, nor any of their employees, nor any of their contractors, subcontractors, or their employees, makes any warranty, express or implied, or assumes any legal liability or responsibility for the accuracy, completeness, or any third party's use or the results of such use of any information, apparatus, product, or process disclosed, or represents that its use would not infringe privately owned rights. Reference herein to any specific commercial product, process, or service by trade name, trademark, manufacturer, or otherwise, does not necessarily constitute or imply its endorsement, recommendation, or favoring by the United States Government or any agency thereof or its contractors or subcontractors. The views and opinions of authors expressed herein do not necessarily state or reflect those of the United States Government or any agency thereof.

Interstrand Resistances in Cored Rutherford-Type Superconducting Cables

Rainer Soika and Arup K. Ghosh*

Superconducting Magnet Division, Brookhaven National Laboratory, Upton, NY, USA

Abstract

The network model of interstrand contact resistances (ICRs) is often used to describe the flow of interstrand coupling currents in Rutherford cables, and to predict the contribution of these currents to the ac losses of such cables. Recent evidence indicates that in cored Rutherford cables, the interstrand resistances are significantly lower in the cable edge region than they are in the flat area of the cable. To investigate these non-uniformities, the VI method was used to determine voltage profiles for cored cables of varying length. The results of the measurements have implications for both the measurement of ICRs via the VI method, and the calculation of ac losses.

Keywords: Interstrand resistance, Cored Rutherford cable, Ac-losses

* Corresponding Author: Tel.: (631) 344 3974,   fax: (631) 344 2590,
Email address: aghosh@bnl.gov

1. Introduction

Rutherford cables, first developed in the 1960s at the Rutherford Appleton Laboratory in the UK, are used frequently in today's accelerator magnets. Over the years, different models describing the flow of coupling currents and predicting ac losses in Rutherford type cables have been put forth. One of the most common models used today is the network model. It evolved from the early work of Morgan [1] at BNL through the work of Sytnikov [2] and Niessen [3] to the work of Verweij [4] at CERN. At CERN it is the model used for the experimental and theoretical treatment of Interstrand Contact Resistances (ICRs) in the extensive development work for the superconducting dipole magnets of the Large Hadron Collider (LHC) [5,6]. Within the framework of the network model, the so-called VI method (also referred to as 'electrical method') is often used to determine the interstrand resistances R_c (crossover resistance) and R_a (adjacent resistance) between different strands in a Rutherford cable.

Interstrand resistances influence the behavior of a superconducting accelerator magnet in many ways, and their optimization is generally a trade-off between different requirements: High ICRs are desirable because for a given induced voltage (driven by dB/dt), higher ICRs lead to smaller induced interstrand coupling currents. This reduces operating costs by lowering ac losses, and is also beneficial in the control of supercurrents or boundary-induced coupling currents, slowly-decaying currents in accelerator magnets that cause significant field distortions. It also helps in stabilizing the magnet as coil heating is suppressed and thus the temperature margin for magnet operation is maintained. Low ICRs on the other hand are desired to allow current sharing between strands, aiding the dynamic stability of the magnet.

Cored Rutherford Cables, first described in 1979 [7], have received renewed attention in recent years [8-10]. Such cored cables distinguish themselves from uncored cables through the

presence of a (normal-conducting or insulating) core between the top and the bottom layer of the cable. Cored cables are attractive because the core significantly increases the crossover resistance R_c while keeping the adjacent resistance R_a low. (Uncored cables do not allow for independent manipulation of R_a and R_c: For a given set of cable parameters, a strand surface treatment that increases R_c also leads to an increase in R_a). The high R_c is the reason for a significant ac loss reduction; this is discussed, for example, in [10-12]. R_a is kept low to allow for current sharing between strands. The cored Rutherford cable samples used in this experimental investigation are Nb-Ti cables under consideration for use in a fast-ramping superconducting synchrotron at GSI Darmstadt, Germany [13]. They use modified RHIC strands, the modification being a shorter wire twist pitch of 4 mm as compared to 13 mm, and the staybrite-coating of the strands. The difference from the RHIC cable design is the core, the dimensions of the cable are identical. In addition to fast-ramping Nb-Ti magnets, cored Rutherford cables are also of interest for Nb_3Sn accelerator magnets of the wind-and-react variety ([8] and [10]), where the Nb_3Sn reaction heat treatment after coil winding often leads to a sintering of the strands, and thus unacceptably low ICRs.

Cored Rutherford cables also allow for a more detailed study of the adjacent resistance R_a. In uncored cables, R_c is often more than an order of magnitude lower than R_a. Thus, current flows predominantly through R_c, making it difficult to gain much insight into R_a. Furthermore, for the RHIC cables, in the case of $R_a = R_c$, the ac loss (for an applied transverse field) associated with R_c is ~ 45 times higher than the loss associated with R_a. Other cable designs show similar ratios. For these reasons, investigations into ICRs for non-cored cables have generally focused on R_c. In cored Rutherford cables, however, R_c is significantly higher than R_a. Thus, it is R_a that

determines the ac losses; and the current paths of interstrand coupling currents are also predominantly governed by R_a.

The correct (or appropriate) choice of sample length has long been debated, both for ICR measurements via the VI-method, as well as for (magnetic or calorimetric) ac loss measurements. The ICR measurements described in [10] use samples that are 100 mm long for a twist pitch length L_p of 73 mm; while [4] uses a length of 3 times L_P. Ref. [8] reports that for their ac loss measurements of samples that had a length L= 90/105·L_p, different authors suggest length correction factors ranging from almost no correction to a correction factor of 3. In this paper, we are presenting VI-method curves of cored Rutherford cables of varying length. The results show significant differences in measured VI profiles as well as their associated interstrand resistances.

2. Background

2.1. The Network Model

As detailed reviews of the network model can be found in the literature, for example [4], we recall only the important features of the model here and refer the reader to the literature for additional information. In the network model, the N strands of a Rutherford cable are assumed to be electrically connected to each other by a network of discrete resistances R_a and R_c. Over the length of a twist pitch L_p, each strand in the cable crosses every other strand in the cable twice, so that there are (2N-2) crossover resistances R_c connected to each strand. As each R_c is connected to two strands, there are (N-1) R_c per strand per L_p. The adjacent resistance R_a in the network model is defined per unit crossover length, and there are (4N) R_a anchored on every strand along the length of a twist pitch: (4N-4) are anchored at the crossover points, and 4 more

R_as are located parallel to the cable at either cable edge. Thus, per strand per L_p there are 2N R_a in the cable. The make-up at the cable edge can be seen in Fig. 1, with a zoom-in given in Fig. 2.

It should be noted that all adjacent resistances R_a connect only adjacent strands, while crossover resistances R_c connect any given strand to all other strands in the cable. This implies that there exist crossover resistances R_c (1 R_c per strand per L_p) that connect a given strand to its adjacent strand. These R_c are located right at the cable edge, as the one shown in Fig. 2. Most importantly, these R_c cannot be distinguished by the VI measurement (or any other measurement) from all the R_a that connect adjacent strands. Furthermore, the core inside a cored cable is located 'between the cable edges'; as it is physically impossible to insert a foil into the region where the strands transition from top to bottom layer (or vice versa). Thus, the R_c at the cable edge has two features that distinguish it from all other R_c: It connects adjacent strands (and thus shows up in the VI voltage profile like an R_a); and, unlike the R_c in the flat cable region, it does not incorporate a core.

This complicated structure of ICRs at the cable edge deserves a few additional words: As it is experimentally impossible to determine whether it is R_a or R_c that transfers current from strand N to strand N+1 in the cable edge region, one has to make a choice as to how to determine the appropriate values for R_c and R_a. We will follow the convention that is suggested by previous work ([9] and [11]) here; that is we will assume R_c in the cable edge region to be as high as it is in the flat (cored) cable region, and assume that the low resistance in the cable edge region is due to R_a. In previous work [9,11], this, along with a modification of the formula for ac losses, was used to predict ac losses for cored Rutherford cables: Ref. [11] measured R_a using the VI method; while Ref. [9] made the correlation between measured ICRs and measured ac losses. [9] modified the expression for ac losses due to R_a in an applied transverse field [14], to account for

R_a being concentrated in the cable edge region: The assumption that R_a is concentrated in the cable edge region leads to a loss enhancement by a factor of three compared to the standard expression, the reason being the increased size of the eddy current loops. The measured values for ac losses then were bracketed by the standard expression for ac losses due to R_a in an applied transverse field, and the modified expression. In keeping with [9] and [11], a high R_c will thus be assumed from here on out. As the average R_c in cored cables is on the order of 10^3 times higher than the average R_a, we will henceforth assume current flow only through R_a; which is the limiting case for $R_c/R_a \rightarrow \infty$.

2.2.   Experimental

The experimental determination of R_c and R_a is generally accomplished via the VI method, as described in detail in [4] or [5]. In short, current is introduced into two opposite strands (1 and N/2 + 1 in an N-strand cable) of the cable test sample and the voltage between strands (relative to one of the current input strands) is measured. Then a voltage versus strand position graph is plotted, commonly for strands 1 through N/2+1, or strands 1 through N+1 (strand N+1 is the same strand as strand 1, after counting through the strands once). From the resulting voltage versus strand profile the magnitude of R_c and R_a can be extracted when the curve is fitted to a profile computed by, for example, the program VIRCAB of Verweij [4]. Such a profile is shown in Fig. 3.

If one assumes that the R_a are constant along the length of the cable, it is established that for $R_c/R_a \rightarrow \infty$, this profile approaches a straight line, and for samples of length L_s, R_a is given by

$$R_a = 8 \cdot \frac{V}{I} \cdot \left(\frac{L_s}{L_p} \right) \tag{1}$$

where V and I are the voltage and current between strands 1 and (N/2+1). (see, for example, [11] and [13].) In cored cables, R_c is typically two to three orders of magnitude larger than R_a. The above formula will underestimate R_a by less than ~ 5 % for $R_c/R_a > 200$ [11]. However, it should be pointed out that equation 1 assumes that the R_a are constant along the cable length, but this is not the case [11]. Thus one measures the average over a number of R_a that are in parallel. To get accurate values for the average R_a (allowing one to predict ac losses properly), it is clearly important that the test sample be made up of a representative number of R_a.

3. Experimental

3.1 Cable and Curing

As noted above, the cable used for the experiments is a Rutherford cable that has parameters identical to those of the RHIC cable, but also features a core. The relevant cable parameters are given in Table I. The cable segments used in this test have been named GSI003-E and have a core consisting of two 8mm wide 25 μm thick stainless steel foils. The 8 mm foil is the widest that can be introduced into the core of the cable during cabling and covers the entire available width of the core of the cable. The cabling was done at New England Electric Wire Corporation (NEEWC), and the cable was then insulated with a double layer of Kapton (50 % overlap) at BNL. The strands in these cables are coated with Staybrite ($Sn_{96\%wt}Ag_{4\%wt}$). The cable stack curing is done according to the RHIC main dipole magnet curing cycle, as described, for example, in [11]. It should be pointed out that while the cable was coated with Staybrite in a manner similar to LHC main dipole procedures (and unlike RHIC, which had bare strands), the RHIC cable stack curing procedure is different from LHC procedures in the release of pressure at the highest temperature. As this is the temperature at which the resistive oxide layers are formed, the result of this step is that there is more surface area of the strands that is being exposed to

oxidation. The outer wrap is coated on the outside with a polyimide adhesive that bonds the different layers of the cable during curing. Because of the keystone angle, the wires are significantly more compacted on the thin side on the cable than they are on the thick side. The compaction on the thin edge is about 18 %, while the compaction on the thick edge of the cable is only about 2 %. For samples of this type of cable, R_c has previously been found to be 62.5 mΩ. This is more than 10^3 times higher than R_a (as will be shown below).

3.2   Experimental Setup

The experimental setup for the measurement of ICRs at BNL consists of a sample holder/sample compression fixture that is immersed in liquid helium. The samples are compressed to 70 MPa via bolts that are torqued to specific values, and are then instrumented with current leads and voltage taps before being immersed in liquid helium. The load versus torque behavior of the fixture is checked periodically with a load cell. The samples were prepared in '10-stacks', so that there were 4 spacer pieces of cable above and below the 2 pieces in the middle of the sample, which were measured. A more detailed description of the RHIC curing cycle and the cable sample preparation is given in [11].

To measure the samples we use a chart recorder to record the voltage versus current characteristics of our samples, ramping from 0 to 100 Amperes, then holding at 100 Amperes and recording the sample voltage. Furthermore, we measured two cable pieces for each individual test as described in the following sections. All measurements on cable samples were made during the same cooldown, to avoid possible changes in interstrand resistance due to thermal cycles. It is our experience from previous measurements at BNL that the interstrand resistances of samples go up after a pressure release and re-torquing and subsequent cooldown. As we were not able to conclude conclusively whether a simple thermal cycle would also change

the interstrand resistances, we circumvented this possible problem by only cooling down once and only testing samples during this one cooldown.

In numbering the strands for the experiments, generally a conveniently located strand was picked and labeled as strand 1, and the other strands were counted clockwise from there (when looking at the cable cross-section on which the current and voltage connections were made).

3.3   Voltage Profile for Sample of Length $L_p/4$

The distinguishing feature of a sample of length $L_p/4$ is that some of the adjacent strands in the sample are compressed over the flat cable region only, while others are compressed over the cable edge region as well as over the flat region (in which case the cable edge resistance, being much lower, dominates the current path). This makes it possible to distinguish between the resistance between adjacent strands in the cable edge region, and the resistance between adjacent strands in the flat cable region. The voltage profiles measured for $L_p/4$ samples were gathered in the 'conventional' VI method manner, however with an additional twist: First, a profile was measured with current being fed into strands 1 and 16, and then (during the same cooldown) a second profile was measured with current being fed into the sample via strands 9 and 24. The two profiles measured for one of the samples can be seen in Fig. 4. It is obvious that their shapes are quite different from each other; the choice of the current input strands significantly influenced the measurement. Furthermore, neither shape resembles any of the known voltage profiles for different ratios of R_a/R_c. The calculated values for Ra (from (1)) are: 287 $\mu\Omega$ (1-16) and 288 $\mu\Omega$ (9-24).

To understand these profiles better we can turn to Fig. 5. It shows the incremental absolute voltage change per strand between strands, referenced to strand 1 [note that in Fig. 3, the 'I-V 1-16' voltage profile starts at strand 1, whereas 'I-V 9-24' profile starts at strand 9. The

incremental changes in voltage seen in 'I-V 9-24' are shifted by 8 strands to the left (or 22 to the right) to plot the profile for the same absolute strand in the sample]. It can be seen that the incremental resistances between strands are quite different for different strands. These differences in resistances are the reason for the voltage profiles being shaped as shown above, and unlike any of the known profiles for different ratios of R_c/R_a. By tracing individual strands, we find that adjacent strands that show low adjacent resistances are strands that are clamped in the cable edge region, where the strands make the transition from 'bottom' to 'top' and vice versa. The wires showing large adjacent resistances are the ones that are clamped only over the flat cable region. This confirms a previous suspicion [11] that the contact resistance is significantly lower in the cable edge region.

3.4   Voltage Profile for Sample of Length $L_p/2$

Two samples of length $L_p/2$ were measured in a manner identical to the $L_p/4$ samples. The graphs for one of these are given in Fig. 6. Here we see the expected pattern for a cable with high R_c (i.e., a profile approaching a straight line). If we use equation (1) to calculate R_a, we get values of 48.4 $\mu\Omega$ (1-16) and 51.2 $\mu\Omega$ (9-24) for the sample shown. Additionally, there is little difference in the shape of the profiles, indicating that the choice of current input strand did not influence the measurement.

3.5   Voltage Profile for Sample of Length L_p

Fig. 7 shows the ICR voltage profile for two samples of length L_p. As was the case for the $L_p/2$ sample, the profile approaches a straight line. Using equation (1), we calculate R_a to be 26 $\mu\Omega$ in both cases. These values are almost a factor of two lower than the ones calculated for the sample of twist pitch length $L_p/2$.

4. Analysis and Discussion

The results show the influence of the sample length on the ICR voltage profile, as well as on the measured value of R_a. The differences between the $L_p/4$ sample on one hand, and the $L_p/2$ and L_p samples on the other, is striking. Despite the fact that the $L_p/2$ and L_p samples exhibit similar voltage profiles, they yield significantly different values for R_a.

A sample length of $L_p/4$ yields a distorted voltage profile, as well as calculated values of R_a that appear artificially high. The low-resistance current path in the cable edge is not correctly incorporated in the measured profile. The discrepancy between the $L_p/2$ and L_p samples deserves further investigation. As can be calculated from Table I, the cable compaction on the thin cable edge is ~ 18 %, while it is only ~ 2 % on the thick cable edge. It is conceivable that the different compactions influence the interstrand resistance in the cable edge region.

5. Conclusion

In Rutherford cables, the interstrand contact resistance in the cable edge region is significantly lower than it is in the flat region of the cable. When measuring R_a (and ICRs in general) via the VI method it is thus important that the sample length be chosen correctly. Evidence suggests that either a sample length of $L_p/2$ or L_p will yield values for R_a that correctly estimate the resistance of ac loss eddy current paths. However, additional work is needed to clarify this situation.

Lengths other than a half-integer multiple of the cable twist pitch length will lead to distortions of the interstrand voltage profile, especially if the cable has $R_c > R_a$ (which is commonly the case for cored cables).

To elucidate the situation, a thorough study and comparison of interstrand resistance measurements and ac loss measurements is necessary. Furthermore, the network model and its application to cored cables also deserves further investigation

Acknowledgement

[1]   Morgan GH. J. Appl. Phys. 1970;41:3673-3679
[2]   Sytnikov VE, Svalov GG, Akopov SG, Peshkov IB. Cryogenics 1989;29:926-930
[3]   Niessen EMJ. Ph.D. Thesis, Twente Univ., 1993
[4]   Verweij AP. Ph.D. Thesis, Twente Univ., 1995
[5]   Richter D, Adam JD, Depond JM, Leroy D, and Oberli LR. DC Measurement of Electrical Contacts between Strands in Superconducting Cables for the LHC Main Magnets, IEEE Trans. Appl. Supercond., vol. 7, no. 2, pp. 786-792, June 1997
[6]   Richter D, Adam JD, Leroy D, and Oberli LR. Strand Coating for the Superconducting Cables of the LHC Main Magnets, IEEE Trans. Appl. Supercond., vol. 9, no. 2, pp. 735-741, June 1999
[7]   Wake D, Gross D, Yamada R and Blatchley B. AC Loss in Energy Doubler Magnets, IEEE Trans. Mag., vol.-15, no. 1, pp141-142, January 1979
[8]   Sumption MD, Collings EW, Scanlan RM, Kim SW, Wake M, Shintomi T, Nijhuis A and ten Kate HJ. AC loss in cored stabrite cables in response to external compaction and variation in core thickness and width, Cryogenics 41 (2001) 733-744
[9]   Wilson MN, Ghosh AK, ten Haken B, Hassenzahl WV, Kaugerts J, Moritz G, Muehle C, den Ouden A, Soika R, Wanderer P, Wessel WAJ. Cored Rutherford Cables for the GSI Fast Ramping Synchrotron, IEEE Trans. Appl. Supercond. vol. 13, no. 2, pp. 1704-1709, June 2003
[10]   Devred A, Bacquart L, Bredy P, Bruzek CE, Laumond Y, Otmani R and Schild T. Interstrand Resistance Measurements on Nb$_3$Sn Rutherford-Type Cables, IEEE Trans. Appl. Supercond., vol. 9, no. 2, pp. 722-726, June 1999
[11]   Soika R, Anerella MD, Ghosh AK, Wanderer P, Wilson MN, Hassenzahl WV, Kaugerts J, and Moritz G. Inter-strand Resistance Measurements in Cored Rutherford Cables, IEEE Trans. Appl. Supercond., vol. 13, no. 2 , pp. 2380-2383 June 2003
[12]   Wilson MN, Moritz G, Anerella M, Ganetis G, Ghosh AK, Hassenzahl WV, Jain A, Joshi P, Kaugerts J, Muehle C, Muratore J, Thomas R, Walther G and Wanderer P. Design Studies on Superconducting Cos θ Magnets for a Fast Pulsed Synchrotron, IEEE Trans. Appl. Supercond., vol. 12, no. 1, pp. 313-316, March 2002
[13]   Moritz G. Superconducting Magnets for the 'International Accelerator Facility for Beams of Ions and Antiprotons' at GSI, IEEE Trans. Appl. Supercond., vol. 13, no. 2, pp. 1329–1334, June 2003
[14]   Wilson MN. Rate Dependent Magnetization in Flat Twisted Superconducting Cables, Internal Report RHEL/M/A26, Rutherford High Energy Physics Laboratory, September 1972
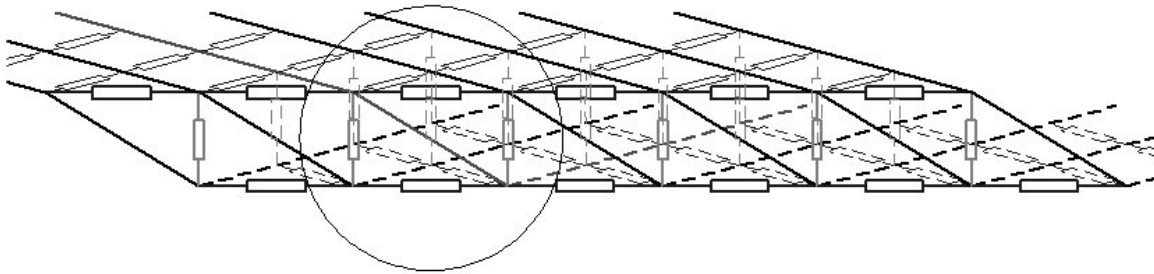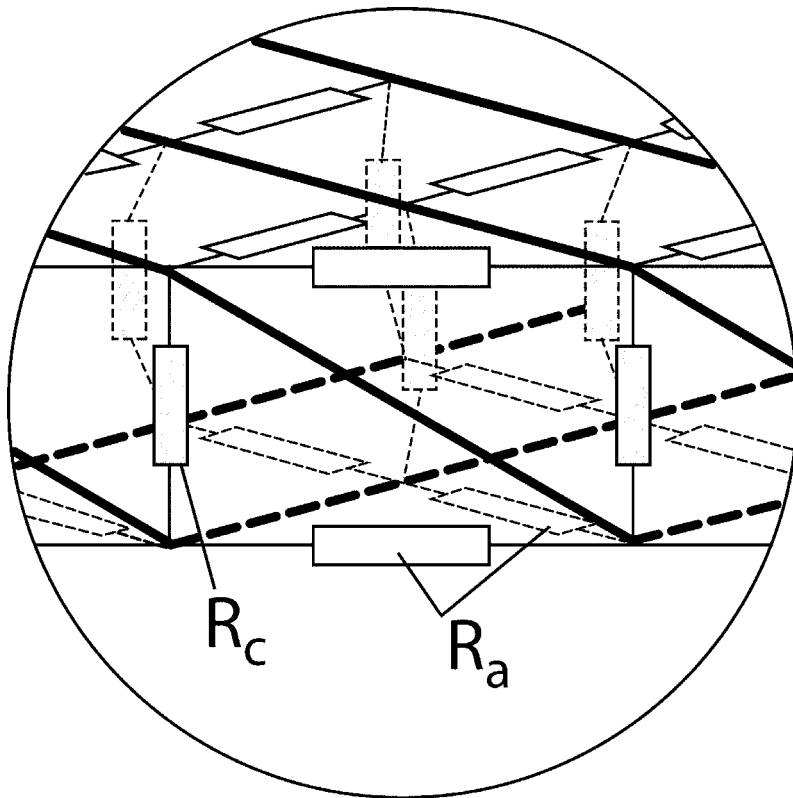
Fig. 1. The Network Model at the cable edge.

Fig. 2. Adjacent resistance R_a (open boxes) and crossover resistance R_c (shaded boxes) at the cable edge.

Table I

GSI/RHIC Cable Parameters

Number of Wires in Cable, N	30
Cable Twist Pitch, L_p	74±5 mm
Cable Mid-Thickness, t	1.166±0.006 mm
Cable Width, w	9.73±0.03 mm
Cable Keystone Angle	1.2±0.1 deg
Wire Diameter, d	0.641 mm
Foil Width	8 mm
Foil Thickness	2·25 μm
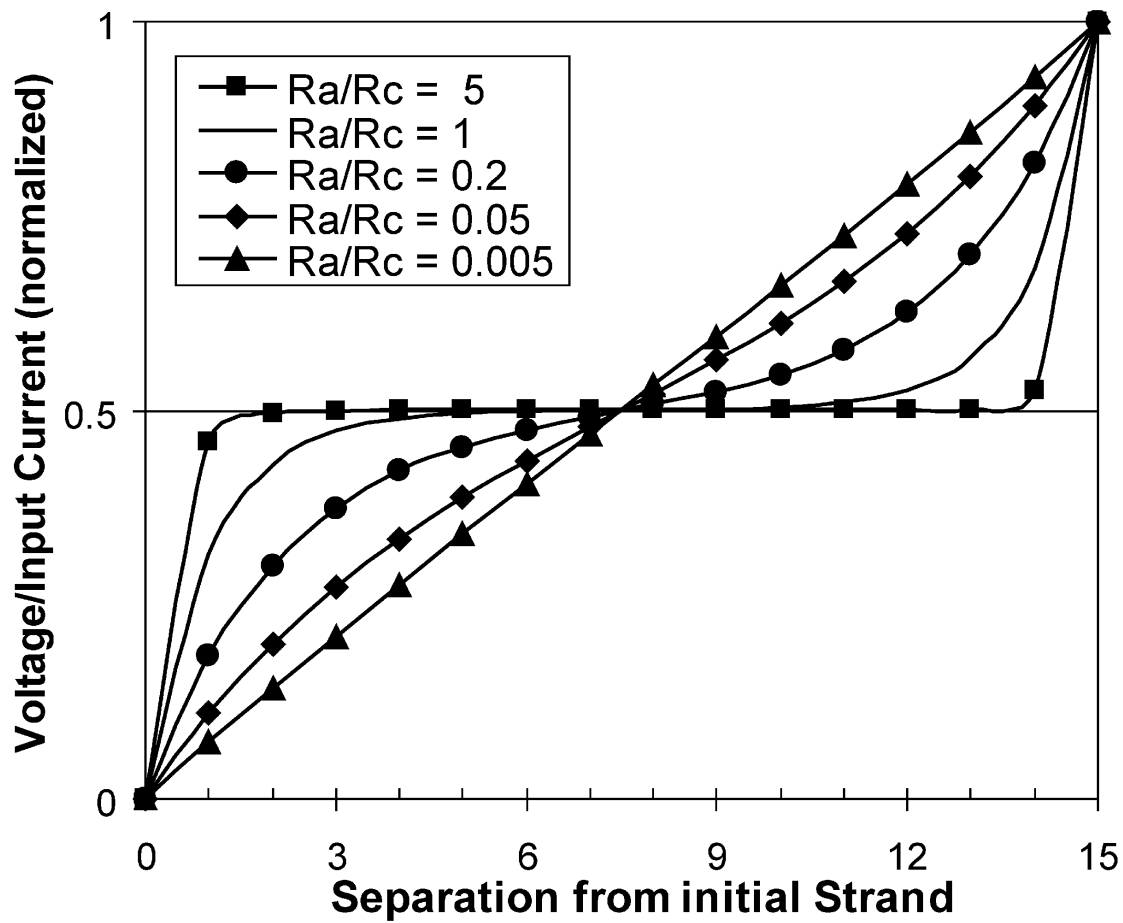
Fig. 3. ICR Voltage Profile for various values of R_a/R_c.
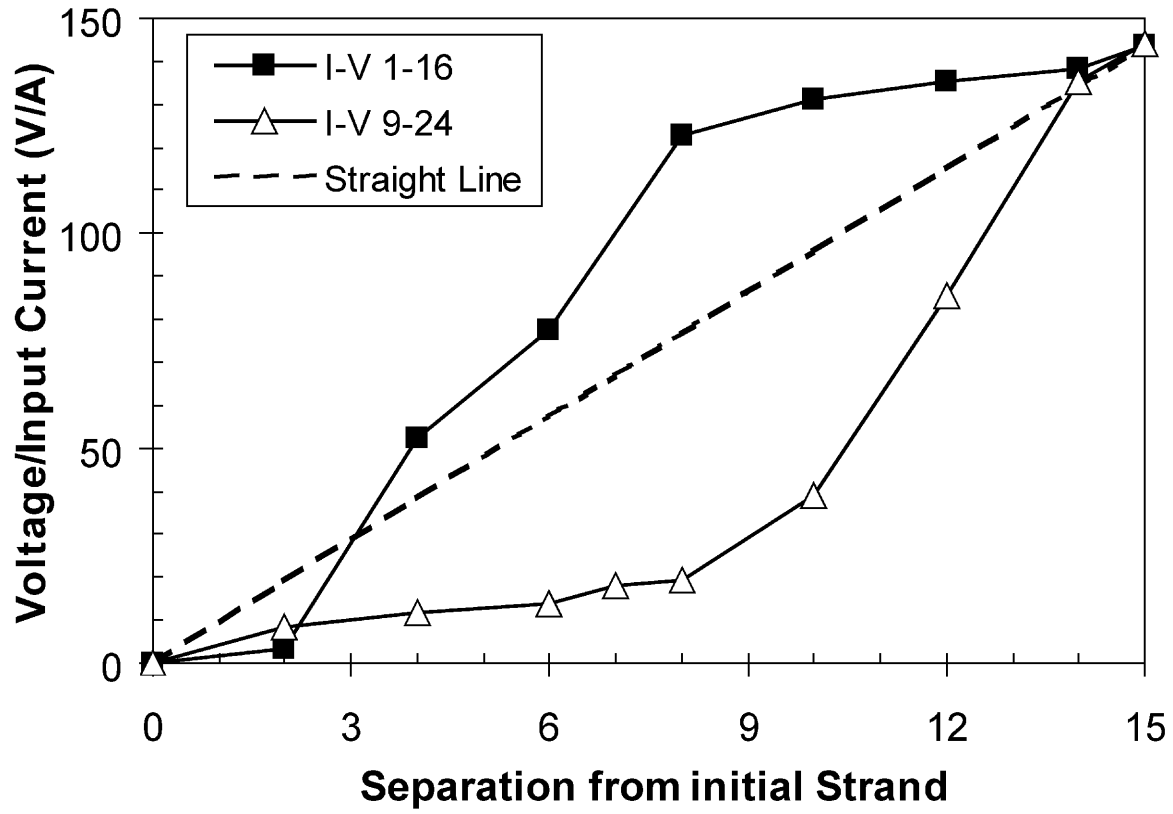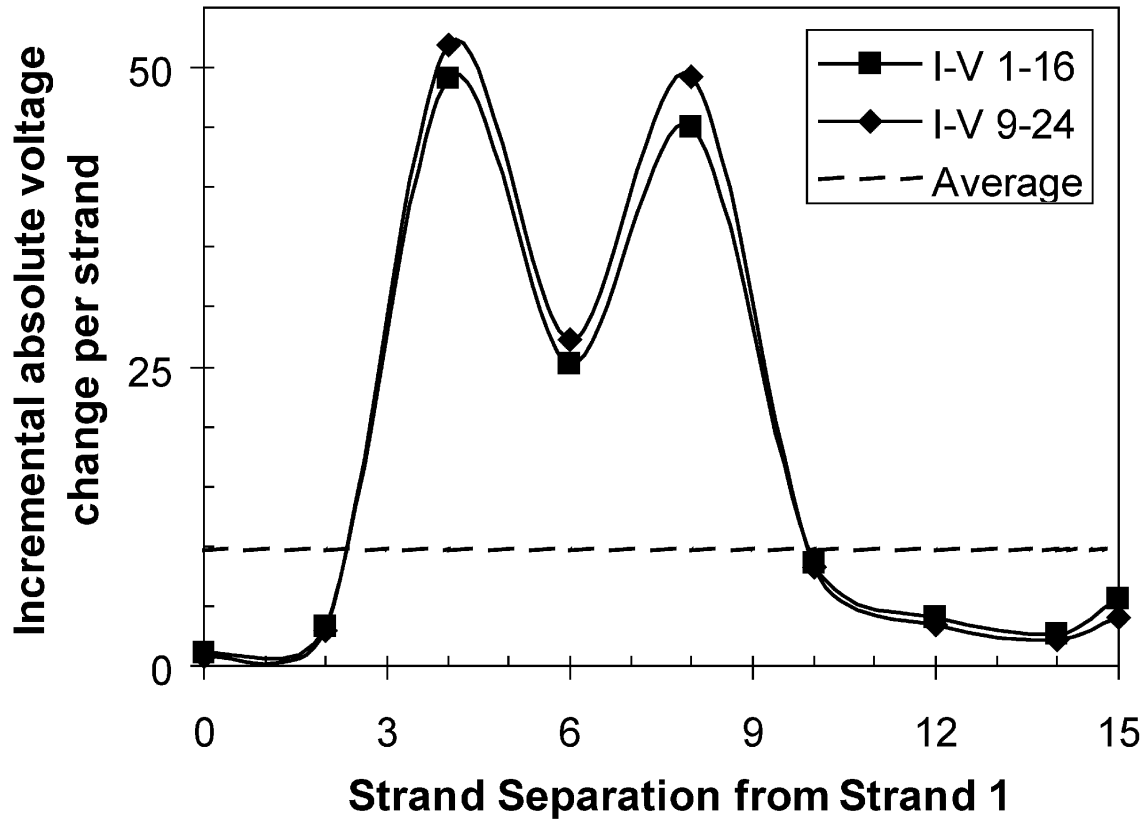
Fig. 4. ICR Voltage Profile for sample of length $L_p/4$.

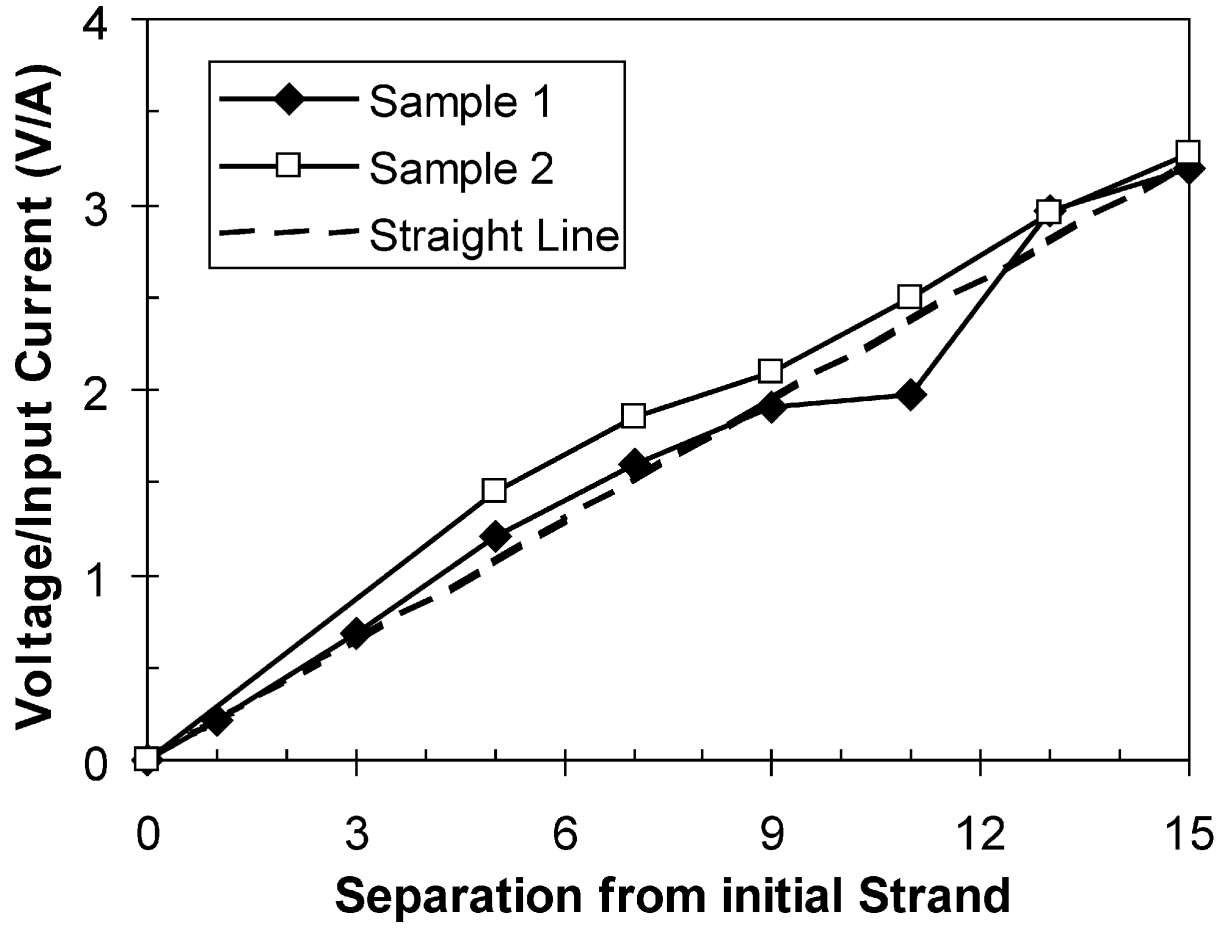Fig. 5. Incremental voltage change for sample of length $L_p/4$.

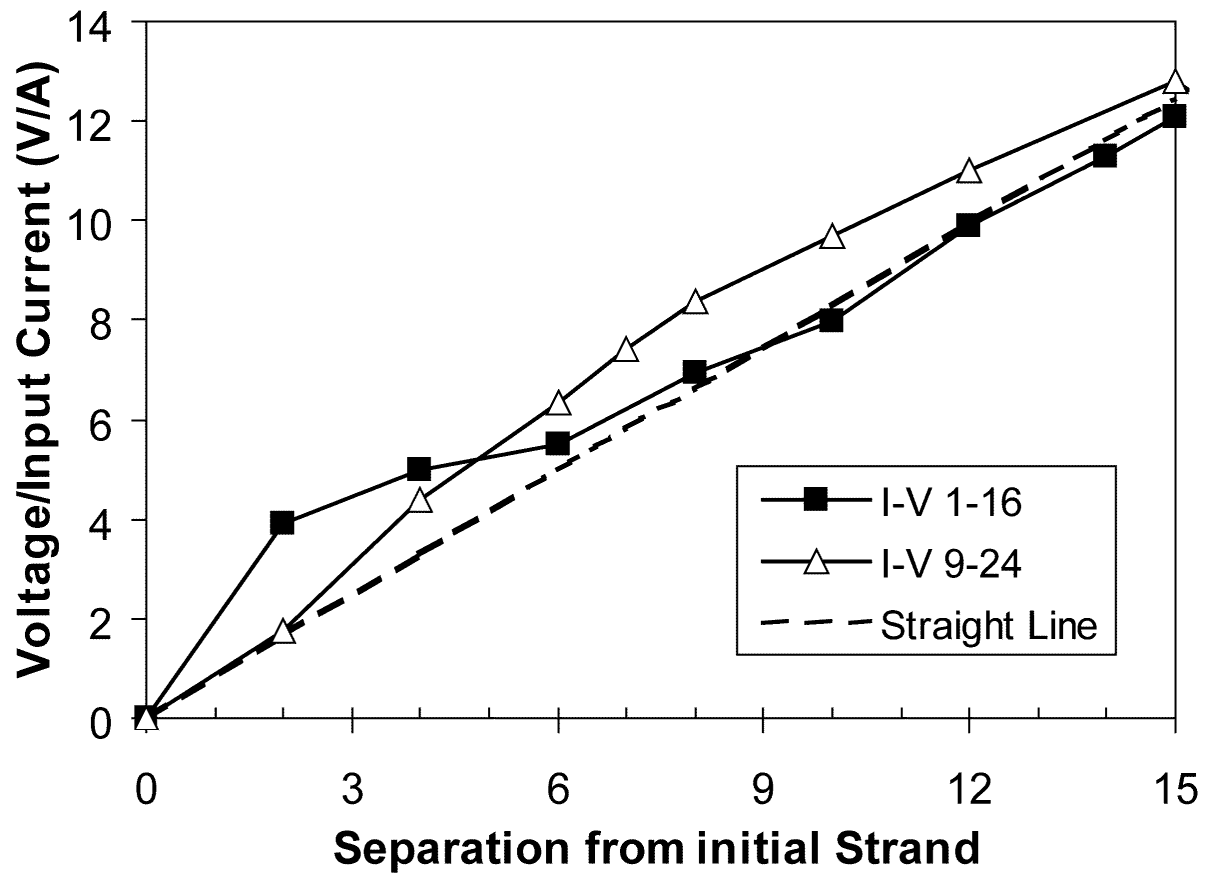Fig.6. ICR Voltage Profile for sample of length $L_p/2$.

Fig. 7. ICR Voltage Profile for sample of length L_p.